^{59}Co NMR Studies of Diamagnetic Porphyrin Complexes in the Solid Phase

Ales Medek, Veronica Frydman, and Lucio Frydman*

Department of Chemistry (M/C 111), University of Illinois at Chicago, 845 W. Taylor Street, Chicago, Illinois 60607-7061

Received: June 23, 1997[⊗]

Solid state ^{59}Co nuclear magnetic resonance (NMR) spectra were recorded on diamagnetic complexes with general structure Co(Por)L_2, where Por = tetraphenylporphyrin, tetramethoxyphenylporphyrin, and octaethylporphyrin; and L = imidazole, methylimidazole, pyridine, and isoquinoline. Measurements were carried out at different magnetic field strengths (4.7, 7.1, and 11.7 T) on both static and spinning samples. Iterative fitting of these data yielded the shielding and quadrupolar parameters that characterize the various cobalt(III) sites in the complexes. These results are only in partial agreement with data inferred from previous solution NMR measurements. The values measured for the anisotropic components of the ^{59}Co NMR tensors also deviate from traditional correlations observed for simpler nonaromatic solid cobalt complexes. Possible sources for the discrepancies observed between the solution and the solid phase parameters as well as for the anomalous behavior observed with the anisotropic ^{59}Co coupling constants are discussed.

1. Introduction

Cobalt complexes constitute important members of the metalloporphyrin family.[1] Hexacoordinated Co(III) porphyrins are isoelectronic and structurally similar to Fe(II) hemins and can therefore be regarded as model systems for understanding the reactivity and redox behavior of these natural compounds. In their own right, complexes between cobalt and porphyrinoid macrocycles play fundamental biological functions related to dehydrogenation and alkyl transfer reactions in vitamin B_{12} and its derivatives.[2] Understanding the electronic properties of cobaltoporphyrins is consequently a topic worth of investigation, in which cobalt NMR can play an important experimental role. With a receptivity that exceeds that of ^{13}C by 3 orders of magnitude, ^{59}Co is a naturally abundant spin susceptible to relatively simple observation. Moreover, cobalt's chemical shift range spans in excess of 10 000 ppm, thus allowing one to monitor even subtle changes in electronic environments.[3] Complicating these NMR measurements is the $S = 7/2$ spin number of ^{59}Co, associated with a moderate quadrupole moment ($Q = 0.42 \times 10^{-24}$ cm^2). In spite of this drawback, numerous ^{59}Co NMR studies of hexacoordinated cobalt complexes in solution have been carried out.[4−7] These analyses have been recently extended to systems in which porphyrins act as the in-plane binding ligands, where the effects introduced by different macrocyclic substitution patterns, different nitrogenated axial ligands, different solvents, concentration, magnetic field, and temperature were explored.[8−12] The ^{59}Co resonance line widths observed throughout these NMR experiments were related via standard relaxation models to the electric field gradients surrounding the metal,[13,14] and the changes observed in their isotropic chemical shifts rationalized using classical paramagnetic shielding models.[15,16]

As is well-known, however, quadrupolar and shielding couplings are not scalar but tensorial properties, best characterized in solids where molecular reorientation are absent.[17] A number of solid phase ^{59}Co NMR studies on relatively simple hexacoordinated complexes have indeed appeared in the literature.[18−23] The present work extends such solid phase ^{59}Co NMR characterizations to a synthetic series of diamagnetic porphyrin complexes involving different macrocyclic substitution patterns and a variety of nitrogenated axial ligands. These measurements were carried out as a function of magnetic field strength and combined with both iterative fitting procedures and analytical calculations, in order to extract the quadrupole and shielding coupling constants of the metal. The values that were obtained in this manner do not correspond with the ones that had been previously inferred from solution data. Anomalies also arose upon attempting to employ standard theoretical models to the correlation of ^{59}Co quadrupolar and shielding anisotropies. These results are discussed in terms of possible limitations of ^{59}Co solution NMR when applied to the study of metalloporphyrins, and of the mechanisms by which the electronic structure dictates the ^{59}Co NMR parameters in this class of compounds.

2. Experimental Section

Materials. Methanol, dichloromethane, chloroform, diethyl ether, and pyridine were purchased anhydrous (Aldrich). Acetone (Aldrich) was distilled from anhydrous calcium sulfate. *N*-methylimidazole (Aldrich) was distilled from BaO. Imidazole, isoquinoline, inorganic salts, and Co(II) porphyrin complexes (Aldrich) were used as supplied. Silicic acid 200−400 mesh (Sigma) was dried at 130 °C for 30 min and allowed to cool in a desiccator over P_2O_5.

Co(III) Porphyrin Complexes: Structure and Preparations. General structures of the hexacoordinated Co(Por)L_2 complexes that were prepared for the present analysis are depicted in Scheme 1. The choice of these model compounds includes variations in the structure of the in-plane macrocycle (tetraphenylporphyrin, tetramethoxyphenylporphyrin, and octaethylporphyrin), as well as in the electronic properties of the axial ligands (imidazole, *N*-methylimidazole, pyridine, and isoquinoline). The first two of these ligands were axially coordinated to all cobaltoporphyrins, while the last two were only coupled to Co(TPP). Co(Por)L_2 complexes were obtained as tetrafluoroborate salts according to the method developed by Balch *et al.*[24] The final products were purified by column chromatography on silicic acid using dichloromethane to remove the less polar impurities, followed by acetone to elute the desired complexes subsequent crystallization was carried out by slow addition of diethyl ether. Positive identification of the final

[⊗] Abstract published in *Advance ACS Abstracts,* October 1, 1997.

S1089-5647(97)02043-9 CCC: $14.00 © 1997 American Chemical Society

SCHEME 1

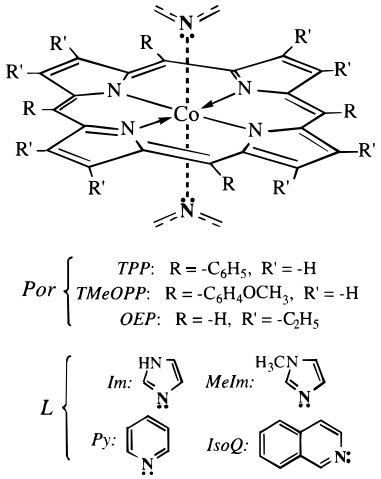

compounds was achieved by means of 200 or 400 MHz ^{1}H NMR and elemental analyses (Midwest Microlab, Indianapolis IN).

NMR Measurements. Solid state NMR determinations were carried out at room temperature using magnetic field strengths of 11.7, 7.1, and 4.7 T, corresponding to ^{59}Co Larmor frequencies of 119.7, 72.5, and 48.0 MHz. Home-built spectrometers and probe heads of similar design were employed in these measurements; all these systems include homodyne radiofrequency (rf) hardware capable of delivering over 1 kW of power to the sample probehead, and Tecmag pulse programmer and software packages for digital control. Various levels of rf irradiation were assayed throughout this study, with solution nutation fields ranging from 20 to 125 kHz. Even for the highest rf power levels the large anisotropic coupling constants characterizing the ^{59}Co complexes restricted most of the spin excitation to the $-^1/_2 \leftrightarrow +^1/_2$ central transition of the Zeeman manifold. High-power ^{1}H decoupling was assayed in preliminary ^{59}Co NMR acquisitions but resulted in no evident line narrowing, and its routine use was consequently discontinued. Spin−lattice relaxation times in most of the analyzed Co(III) complexes were in the order of 10^{-1} s, thus allowing us to use relatively short recycle delays (300 ms) and enabling the averaging of large numbers of scans when necessary. All ^{59}Co NMR spectra were externally referenced using 1 M aqueous $[Co(NH_3)_6]Cl_3$ solutions and subsequently converted to ppm downfield from the 1 M aqueous $K_3[Co(CN)_6]$ resonance position for the sake of consistency with the literature.

Although structurally similar to one another, the cobalt complexes analyzed throughout this study presented marked differences in their quadrupole coupling parameters. This led us to pursue two different spectroscopic strategies in their analyses. When coupling constants were relatively small ($e^2qQ/h \leq 6$ MHz), magic-angle spinning (MAS) was found to be an important aid both toward the interpretation of spectra and as a mechanism of signal-to-noise enhancement; its use was consequently pursued at a variety of spinning rates. As e^2qQ/h increased and second-order quadrupole effects become important the MAS NMR spectra became overly complex, and a static sample approach proved substantially more amenable to analysis. Dead time problems were dealt with in these static experiments by using spin echo sequences in combination with an appropriate phase cycling. Two additional phenomena complicated the retrieval of undistorted powder patterns in these large e^2qQ/h cases: the large line widths of the bands, comparable to the width of the rf excitation profile, and strong nutation effects that introduced an orientation-dependent excitation of the spins. The first problem was eliminated by suitably coadding into the final line shape several powder patterns collected at different transmitter offsets. Nutation distortions were dealt with by employing low excitation powers and short (≈ 1 μs) excitation pulses, so as to provide spins in different crystallites with identical nutation frequencies.[25,26] These precautions allowed us to obtain undistorted NMR powder line shapes, as corroborated by preliminary analyses on model compounds. Echo strategies were also attempted in the MAS experiments but they resulted in severe signal-to-noise losses; even in the absence of this refocusing our relatively short dead times (≈ 15 μs) resulted in only minor spectral distortions which could be compensated by linear phase correction and baseline fix algorithms.

3. Solid Phase ^{59}Co NMR: Basic Considerations

Before presenting the results obtained on the porphyrin complexes, it is convenient to briefly dwell on the parameters that affect line shapes in solid phase ^{59}Co NMR and to summarize the strategies that were adopted for extracting these parameters. As mentioned earlier, ^{59}Co NMR signals are defined by locally induced magnetic fields (chemical shifts) and by the interaction between the ^{59}Co nucleus and its surrounding electronic gradients. Although smaller than the Zeeman interaction, these quadrupole effects are usually too large to be appropriately described by the first term in a Zeeman-based perturbative expansion; inclusion of a second term remedies this deficiency and leads to an overall rotating frame Hamiltonian[13]

$$H_{\text{total}} = H_{\text{q}}^{(1)} + H_{\text{cs}}^{(1)} + H_{\text{q}}^{(2)} \tag{1}$$

where subscripts indicate the nature of the interactions and superscripts denote their hierachy in the perturbative expansion. The dominant term in this expression is usually the first order quadrupolar coupling $H_{\text{q}}^{(1)}$, whose quadratic dependence on the S_z operator endows all single quantum transitions except the $-1/2 \leftrightarrow +1/2$ one with an anisotropy proportional to e^2qQ/h (i.e., with megahertz line widths). This makes the observation of these satellite transitions difficult or impossible, and only the remaining central transitions were detected throughout the present study. The line shapes of these spectra are then given by a first-order chemical shift proportional to the Larmor frequency ν_0

$$H_{\text{cs}}^{(1)} = \nu_0[\delta_{\text{cs}}^{\text{iso}} + \delta_{\text{cs}}^{\text{aniso}}(\theta_{\text{cs}}, \varphi_{\text{cs}})]S_{\text{z}} \tag{2}$$

as well as by second-order quadrupole effects

$$H_{\text{q}}^{(2)} = \frac{(e^2qQ/h)^2}{\nu_0}[\delta_{\text{q}}^{(\text{iso},2)} + \delta_{\text{q}}^{(\text{aniso},2)}(\theta_{\text{q}},\varphi_{\text{q}})]S_{\text{z}} \tag{3}$$

proportional to the square to the quadrupole coupling e^2qQ/h and inversely proportional to the applied field B_0. $H_{\text{cs}}^{(1)}$ and $H_{\text{q}}^{(2)}$ combine to yield central transition spectra that are centered at the sum of isotropic chemical plus quadrupolar shifts and broadened by anisotropic shielding and second-order quadrupole effects. The exact expressions defining these various contributions in terms of the quadrupolar coupling parameters, the chemical shifts, and the Euler angles relating these two tensors have been discussed elsewhere.[27−29]

In principle, these various NMR parameters can be best measured from ^{59}Co spectra recorded on static samples as a function of the external magnetic field strength, as then the different ν_0 dependences shown by $H_{\text{q}}^{(2)}$ and $H_{\text{cs}}^{(1)}$ allow one to remove several ambiguities regarding these couplings that

usually remain after single B_0 determinations. In spite of its generality, this variable-field static NMR approach becomes unsuitable for determining small quadrupole coupling constants in the presence of dominating shielding anisotropies. This complication, although unusual, arose in several of the porphyrin complexes that were analyzed in this study, and it was dealt with by the use of MAS. If performed sufficiently fast, this procedure will scale the relatively small residual quadrupole effects and remove broadenings arising from shielding and dipolar interactions, thus breaking the broad ^{59}Co NMR patterns into manifolds of sharp spinning sidebands. Recording such spectra as a function of spinning speed yields an accurate estimate of a site's isotropic centerband, whose position is given by

$$\delta_{\text{centerband}} = \delta_{\text{cs}}^{\text{iso}} + \frac{(e^2qQ/h)^2}{\nu_0^2}\delta_{\text{q}}^{(\text{iso},2)} \qquad (4)$$

When monitored as a function of ν_0 these well-defined centerband frequencies allow one to obtain accurate estimates of even small quadrupole coupling contributions, as well as the values of the solid state isotropic chemical shifts. Reliable information about the shielding anisotropy of each cobalt site can also be extracted from these data by simulating the MAS sideband patterns observed at various spinning rates and magnetic fields.[30−32] The resulting sideband line shapes actually depend on the three chemical shift tensor parameters, on two quadrupole parameters (e^2qQ/h, η_q), and on the relative orientation between the shielding and quadrupolar tensors. Rather than implementing a full fit of these sideband patterns by numerically searching for the optimum values of these eight parameters it was assumed that the asymmetries of the shift and quadrupolar tensors were equal and that their orientations were coincident. Given the *a priori* determination of the isotropic shifts from the centerband positions, this left the shielding anisotropy and its asymmetry parameter as the only unknown variables remaining in the MAS data simulations.

4. Results

An interesting feature of all the imidazole and *N*-methylimidazole complexes that were analyzed was the observation of surprisingly small ^{59}Co quadrupole coupling constants, which prompted their study by the variable speed MAS method described above. The left-hand columns of Figures 1 and 2 illustrate typical solid state ^{59}Co NMR data arising from these hexacoordinated complexes, using Co(TMeOPP)MeIm$_2$ as an example. This variable spinning speed procedure lead to accurate determinations of the isotropic centerbands at different fields whose difference, although small, allowed us to estimate the relative sizes of the isotropic chemical and quadrupolar shifts (Table 1). Furthermore given the relatively high axial symmetry of the Co(III) complexes η_q can be assumed close to zero, and a coupling constant value $e^2qQ/h = 5.5\pm1.4$ MHz is then inferred. This quadrupolar coupling constant is too small to explain by itself the spinning sideband patterns that are observed in the ^{59}Co MAS NMR spectra, whose shapes are in fact characteristic of shielding-derived anisotropic patterns.[30,33] The selection of an appropriate set of shift anisotropy parameters can indeed reproduce simultaneously all the features observed in the variable-speed/variable-field set of spectra, as illustrated by the simulations presented in the right-hand columns of Figures 1 and 2.

As shown by the high-speed data in Figures 3 and 4, a similar behavior was observed for the remaining Co(III) porphyrin complexes coordinated to imidazole and *N*-methylimidazole ligands. In all cases, MAS NMR detected only one inequivalent cobalt site in the solid, together with substantial sideband manifolds characteristic of shielding anisotropy. Small but reproducible shifts were measured for the centerband positions in the 4.7 and 7.1 T experiments (Table 1) from which the isotropic chemical shifts and quadrupole coupling constants could be estimated. Also reported in Table 1 are the ^{59}Co solution NMR parameters measured for the various compounds analyzed in the present work (chemical shifts and resonance line widths), together with very similar values reported in earlier studies. In order to convey an idea on the reliability of this variable-field MAS NMR method of analysis, the parameters that this approach yields for what can be considered as the parent compound of this series, $[Co(NH_3)_6]Cl_3$, are also reported and compared with literature values. The right-hand columns of Figures 3 and 4 show best fits of the different experimental ^{59}Co sideband patterns to simulated MAS spectra. Very good agreement was obtained in all cases between simulated and experimental data sets using nearly symmetric sets of shielding anisotropy parameters (Table 2), with the only minor discrepancies resulting from the spinning sideband manifolds arising from ^{59}Co satellite transitions. It is worth noting that given the small values observed for the ^{59}Co quadrupolar coupling constants, essentially identical sideband patterns would have resulted even if noncoincident coupling tensors or arbitrary values of η_q were assumed.

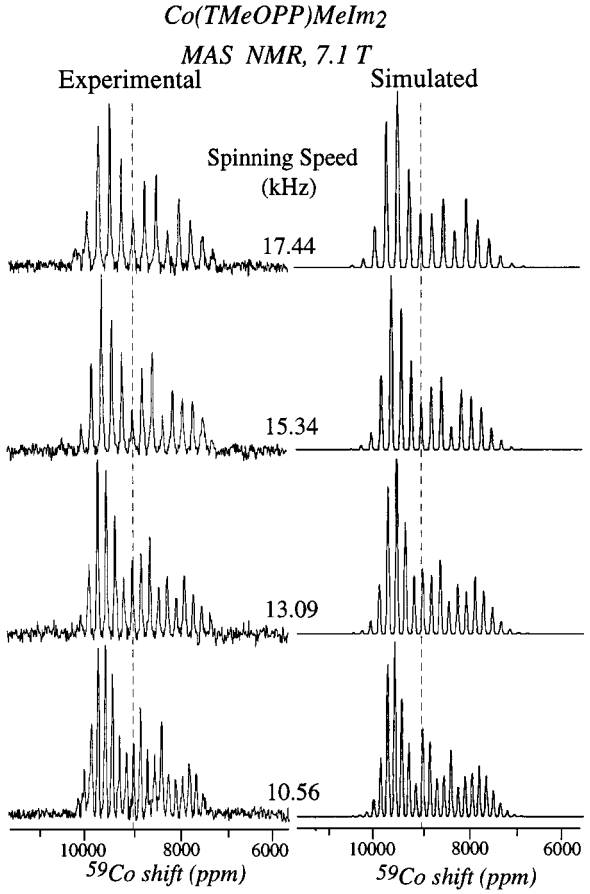

Figure 1. Left-hand column: ^{59}Co MAS NMR spectra of Co(TMeOPP)MeIm$_2$ recorded at 7.1 T using the indicated spinning rates. An average of 3000 scans separated by 300 ms repetition delays were collected for each trace, using a ±250 kHz spectral width and a 1.024 ms single-scan digitization time. The dashed vertical line indicates the position of the isotropic centerband. Right-hand column: Simulated sideband patterns calculated using the shielding and quadrupolar parameters listed for Co(TMeOPP)MeIm$_2$ in Tables 1 and 2, under the assumptions described in the text and for the spinning rates shown in the figure.

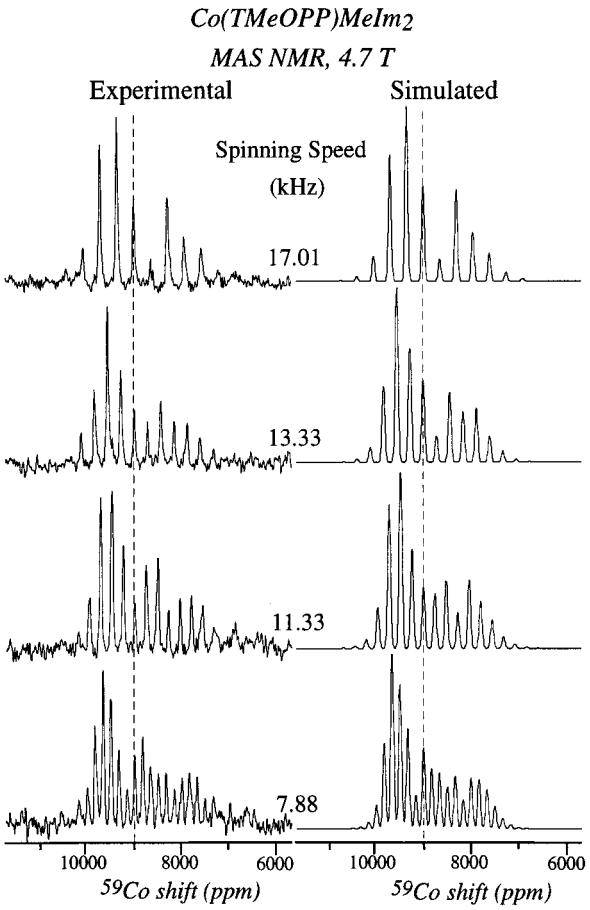

Figure 2. Left-hand column: ^{59}Co MAS NMR spectra recorded on Co(TMeOPP)MeIm$_2$ at 4.7 T using the indicated spinning rates and acquisition parameters similar to those given in Figure 1. The dashed line marks the position of the centerband. Right-hand column: Simulated spectra obtained as described in Figure 1.

In addition to these analyses on imidazole and *N*-methylimidazole derivatives, information was sought regarding the effects introduced by pyridine and isoquinoline ligands on the ^{59}Co NMR parameters of porphyrin complexes. In the case of tetraphenylporphyrin both ligands lead to similar solution ^{59}Co NMR spectra, with resonances shifted slightly upfield and over 20 times broader than those arising from the imidazole analogs (Table 1). No ^{59}Co MAS NMR spectrum could be obtained from Co(TPP)IsoQ$_2$ even after several days of signal acquisition, and only qualitative MAS NMR spectra could be retrieved from the pyridine derivative (Figure 5). These spectra consist of overlapping sets of spinning sidebands whose quantitative analysis is complicated by the presence of second-order quadrupole effects. No such complications arise upon recording the ^{59}Co NMR spectrum of Co(TPP)Py$_2$ on a static powder (Figure 6). Although this trace shows a significant field dependence, it can still be accurately reproduced using a single set of coincident and nearly axially symmetric quadrupole and shielding tensors thus justifying the assumptions that were used in the MAS data simulations. A similar analysis is feasible for the static ^{59}Co NMR spectrum acquired on Co(TPP)IsoQ$_2$ at different magnetic fields (Figure 7); notice that in spite of the substantial quadrupole and shielding broadenings affecting the cobalt resonance of this complex (line widths in excess of 5000 ppm), simulation of its powder line shapes is made possible by the experimental precautions employed in its acquisition.

5. Discussion

Although an ideal discussion of the quadrupolar and shielding results presented in the preceding section should involve quantum chemical calculations relating these observables to molecular structures, no theoretical tools of sufficient reliability are to our knowledge available for dealing with transition metals inserted in systems of such high chemical complexity as porphyrins. In the absence of this computational complement we attempted to analyze the ^{59}Co NMR information in terms of simpler models which have proven useful in the analysis of small transition metal complexes. Shielding parameters in such systems have been traditionally rationalized in terms of paramagnetic contributions, which for diamagnetic Co(III) compounds are usually dominated by the electronic mixing between ground $(t_{2g})^6$ configurations and $(t_2g)^5e_g$ excited states.[3−6,15,16,34] Given the well-defined symmetry of these orbitals the paramagnetic ^{59}Co shielding tensor elements can be described as[35−37]

$$\sigma^{p}_{\alpha\beta} = \frac{\mu_0}{4\pi}\frac{e^2}{2m^2}\frac{1}{\langle \Delta E\rangle_{\alpha\beta}}\langle r^{-3}\rangle_{3d}(D)_{\alpha\beta} \qquad (5)$$

where $\langle \Delta E\rangle$ is the average transition energy between orbitals coupled by the angular momentum operators (L_α,L_β), r is the mean electronic distance from the nucleus, and $(D)_{\alpha\beta}$ reflects an electron imbalance defined by the occupancy numbers of the coupled d orbitals. This equation lies at the basis of well-documented solution NMR analyses which correlate ^{59}Co shifts with optical transition wavelengths related to $\langle \Delta E\rangle$ (spectrochemical effects), and with radial orbital changes brought about by the ligands (nephelauxetism). At a similar level of complexity, another well-documented approach, the Townes−Dailey model, allows one to relate the magnitude of electric field gradients at the metal site with orbital occupancy parameters.[38,39] This method predicts a linear dependence of e^2qQ/h on the D_{zz} and $\langle r^{-3}\rangle_{3d}$ parameters appearing in eq 5, and a good correlation has indeed been observed between the size of the shielding anisotropy and the magnitude of quadrupole coupling constants in several solid cobalt complexes and clusters.[3,18,22,40]

This type of analysis, involving the rationalization of ^{59}Co NMR parameters in terms of crystal field splittings and partial d-orbital populations, has been employed in the interpretation of ^{59}Co NMR data acquired on hexacoordinated cobaltoporphyrins in solution.[8,12] Isotropic versions of eq 5 were employed to characterize the electronic properties of the axial and in-plane ligands; ^{59}Co solution line-width determinations were also coupled to independent correlation time measurements and used to estimate electric field gradient parameters that backed up the chemical shift information. We had expected the present solid state NMR study to become an extension of these solution determinations that would corroborate and help extend previous estimations about the electronic structure of these complexes. Nevertheless significant discrepancies arose when the anisotropic coupling constants that could be inferred from solution NMR were compared with the corresponding parameters measured in the solid. Given the correlation time $\tau_c \approx (1.0-1.5) \times 10^{-10}$ s that had been determined for the porphyrin complexes in solution, the experimental liquid-state ^{59}Co line widths lead to quadrupolar coupling constants of ca. 9 MHz for the imidazole and 35 MHz for the pyridine derivatives.[11] The spectra presented in Figures 1−6, however, unambiguously indicate that much smaller values characterize these quadrupole couplings at the metal sites. Discrepancies also arise upon comparing the information afforded by solution and solid phase NMR regarding the ^{59}Co chemical shift anisotropy: whereas the former technique shows that ^{59}Co relaxation times are independent of the

TABLE 1: Solid and Solution Phase ^{59}Co NMR Parameters Measured for Different Porphyrin Complexes[a]

	solid phase				solution[b] (lit. values[d])	
compound	$\delta_{centerband}^{MAS}$ (ppm, 4.7 T)	$\delta_{centerband}^{MAS}$ (ppm, 7.1 T)	$(e^2qQ/h)/[1+\eta_q^2/3]^{1/2}$ [c] (MHz)	δ_{cs}^{iso}[c] (ppm)	δ_{cs}^{iso} (ppm)	line width (Hz)
Co(TPP)Im_2[e]	8913 ± 3	8928 ± 2	4.9 ± 1.5	8940 ± 6	8344 (8352)	450 (356)
Co(TPP)$MeIm_2$[e]	8621 ± 3	8627 ± 2	3.1 ± 2.4	8632 ± 6	8400 (8410)	660 (523)
Co(OEP)Im_2[e]	9175 ± 3	9200 ± 2	6.4 ± 1.2	9220 ± 6	8814 (8821)	125 (103)
Co(OEP)$MeIm_2$[e]	9014 ± 3	9021 ± 2	3.4 ± 2.2	9027 ± 6	8877 (8886)	230 (190)
Co(TMeOPP)Im_2[e]	8908 ± 3	8921 ± 2	4.4 ± 1.7	8931 ± 6	8372	760
Co(TMeOPP)$MeIm_2$[e]	8995 ± 3	9008 ± 2	5.5 ± 1.4	9023 ± 1.4	8415	1050
	7830 ± 2	7840 ± 1	4.0 ± 1.2 (3.4[g])	7848 ± 2		
$[Co(NH_3)_6]Cl_3$[e,f]	7892 ± 2	7897 ± 1	2.2 ± 1.8 (1.0[g])	7899 ± 2	8180[h]	140[h]
	7954 ± 2	7960 ± 1	2.5 ± 1.8 (2.1[g])	7963 ± 2		
Co(TPP)Py_2[i]			16.5 ± 1	8435 ± 50	8095 (8109)	12000 (12000)
Co(TPP)$IsoQ_2$[i]			26.2 ± 2	8260 ± 50	8143	16600

[a] All shifts externally referenced to $\delta_{K_3[Co(CN)_6]} = 0$ ppm. [b] Measured in acetone using 10 mg/mL concentrations. [c] Error margins propagated from centerband errors or static line shape fits. [d] From ref 10. [e] From MAS measurements, with error margins estimated from line widths and maxima positions throughout the variable-rate series. [f] Multiple sites in the crystal. [g] From single-crystal report, ref 20. [h] Aqueous solution data. [i] From static sample measurements.

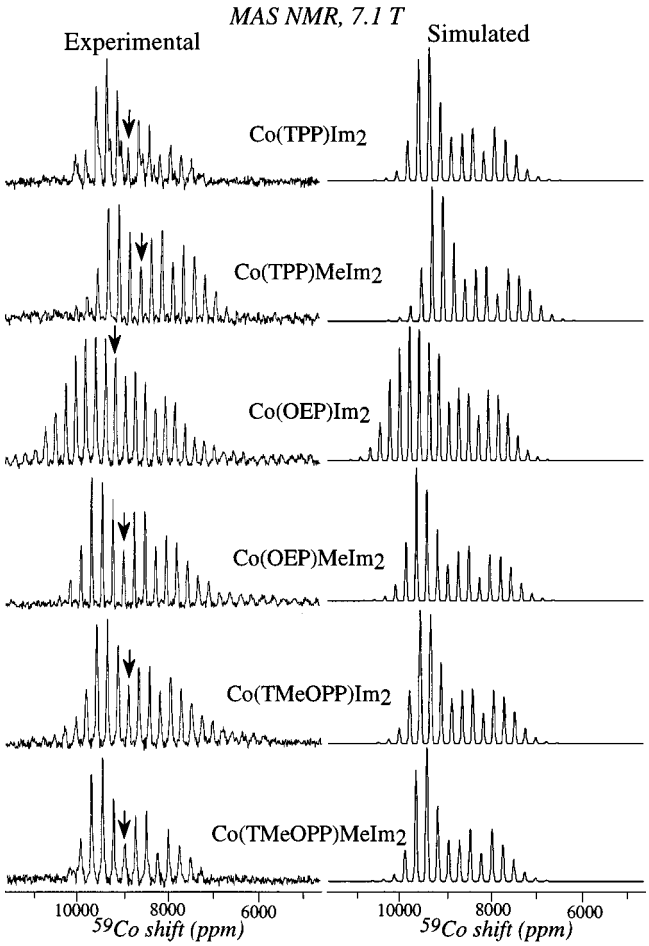

Figure 3. Left-hand column: ^{59}Co MAS NMR spectra obtained for different imidazole and *N*-methylimidazole porphyrin complexes at 7.1 T. Spinning rates employed in these acquisitions ranged between 15.8 and 17.5 kHz; other experimental parameters were as described in Figure 1. Arrows indicate the position of the centerbands identified by variable spinning speed determinations. Right-hand column: Simulated sideband spectra calculated for each compound using the procedure described in Figure 1 and the shielding/quadrupole parameters listed in Tables 1 and 2.

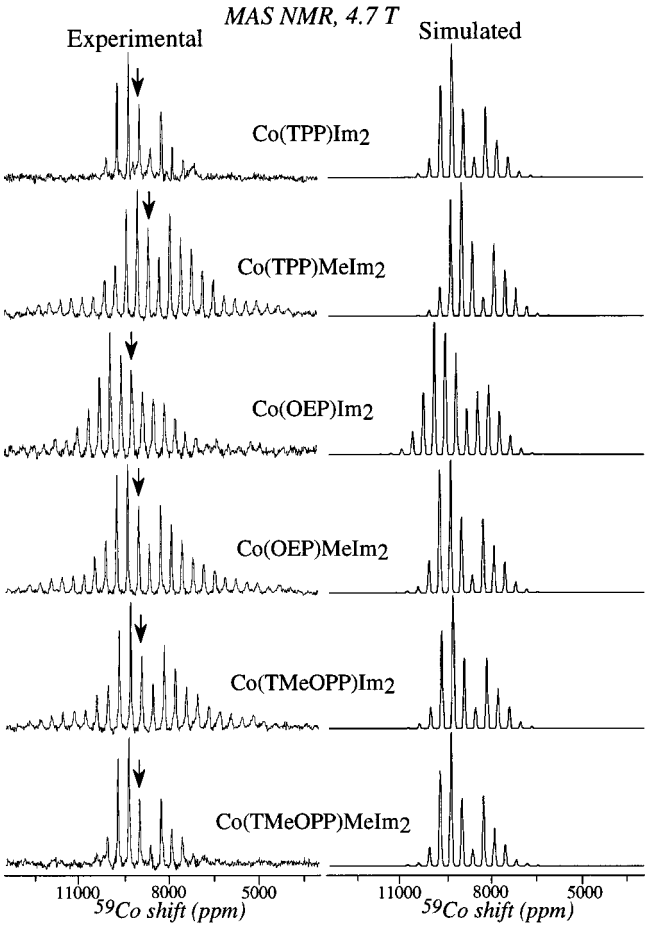

Figure 4. Comparison between experimental and simulated ^{59}Co NMR line shapes obtained for the indicated cobaltoporphyrins at 4.7 T. Spinning rates employed in these acquisitions ranged between 17.0 and 18.0 kHz; other details are as in Figure 3.

applied field and therefore essentially free from shielding anisotropy contributions,[9] the latter reveals substantial shielding tensors that in all cases span a nearly 3000 ppm range. These discrepancies could be reflecting changes in the cobalt chemical environments that occur as complexes go from the crystalline into the solution phase or, as it has been recently suggested, they could arise as a consequence of inaccuracies in the models employed for the analysis of solution ^{59}Co relaxation data in general and of cobaltoporphyrins in particular.[41,42] In any case it is worth noting that in spite of the differences observed between the solution ^{59}Co NMR results and the parameters that we measured in the solid, there is a close agreement between the latter values and similar coupling parameters determined on isoelectronic Fe(II) derivatives by Mossbauer spectroscopy. Room temperature determinations on Fe(TPP)Py_2 powders for instance revealed that the metal site in this complex possesses a quadrupolar splitting of 1.22 mm/s corresponding to an e^2qQ/h value of 14.2 MHz,[43] a coupling that is remarkably close to the one suggested by the simulations in Figure 6.

TABLE 2: Solid Phase ^{59}Co Shielding Tensor Parameters Measured on Co(Por)L_2 Complexes[a]

compound	δ_{cs}^{xx} (ppm)	δ_{cs}^{yy} (ppm)	δ_{cs}^{zz} (ppm)
Co(TPP)Im_2	9915	9630	7275
Co(TPP)$MeIm_2$	9685	9335	6875
Co(OEP)Im_2	10640	9690	7330
Co(OEP)$MeIm_2$	10065	9795	7220
Co(TMeOPP)Im_2	9975	9600	7215
Co(TMeOPP)$MeIm_2$	9930	9765	7375
Co(TPP)Py_2	9450	9270	6590
Co(TPP)$IsoQ_2$	9880	9150	5760

[a] Data considered accurate within ±50 ppm. Elements defined according to the conventions $|\delta_{cs}^{zz} - \delta_{cs}^{iso}| \geq |\delta_{cs}^{xx} - \delta_{cs}^{iso}| \geq |\delta_{cs}^{yy} - \delta_{cs}^{iso}|$; $\delta_{cs}^{iso} = (\delta_{cs}^{xx} + \delta_{cs}^{yy} + \delta_{cs}^{zz})/3$.

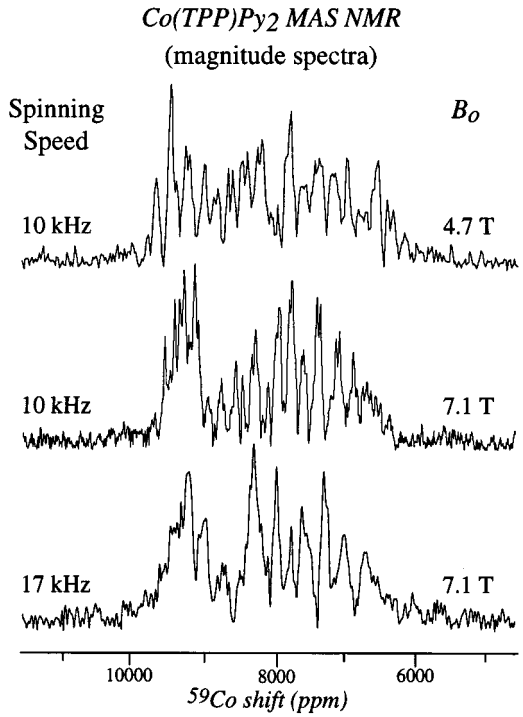

Figure 5. Experimental ^{59}Co MAS NMR spectra obtained for Co(TPP)Py_2 at the indicated B_0 fields and sample spinning rates. Acquisition parameters comparable to the ones described in Figure 1 were employed, albeit with a number of scans in excess of 10^6; the 4.7 T data, for instance, involved 4 days of continuous signal averaging.

Regardless of the discrepancies between the NMR parameters inferred from solutions and those that we have directly measured in the solid, it should be possibly to employ "atom in a molecule" formalisms of the type described above in order to extract from the new NMR couplings the d orbtial occupancies and crystal field splittings characterizing the different complexes. There are strong indications, however, that even though verified for a majority of simple Co(III) compounds, these procedures may lead to unjustified conclusions for more complex systems such as cobaltoporphyrins. Indeed as was mentioned earlier, eq 5 and the Townes−Daily formalism predict a proportionality between the asymmetry of the NMR parameters as viewed by the ^{59}Co electric field gradients and by the shielding anisotropy. A literature survey of e^2qQ/h and shielding anisotropies for simple hexacoordinated cobalt complexes corroborates a good correlation between these two values (Table 3, top). Given the trends that are set by these literature values and the chemical shift tensors that we observe for the solid cobaltoporphyrins, this model predicts that quadrupole coupling constants in these aromatic complexes should fall in the 30−70 MHz range. These predictions overestimate by almost an order of magnitude the experimental values that we measure. A possible explanation

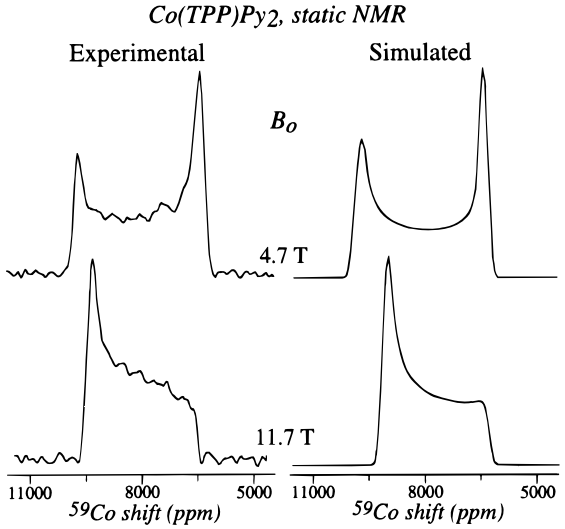

Figure 6. Left-hand column: Static ^{59}Co NMR spectra of Co(TPP)Py_2 recorded at the indicated B_0 fields using a two-pulse spin echo sequence (echo time = 50 μs) and approximately 1.2×10^6 scans. The 4.7 T spectrum is the result of coadding three frequency-shifted patterns, while the 11.7 T spectrum involved five frequency-shifted experiments. Right-hand column: Best fit simulations of the field-dependent powder spectra resulting from $e^2qQ/h = 16.5$ MHz, $\eta_q = 0.1$, the shielding parameters listed in Table 2, and coincident tensor orientations.

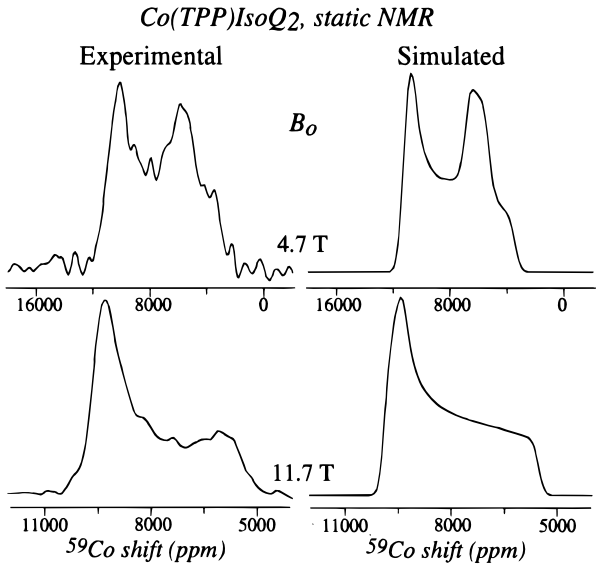

Figure 7. Left-hand column: Static ^{59}Co NMR spectra of Co(TPP)$IsoQ_2$ recorded at the indicated B_0 fields. Experimental conditions were similar to those reported in Figure 6, although approximately twice as many scans and number of offset acquisitions had to be used. Right-hand column: Best fit simulations of the experimental data resulting from $e^2qQ/h = 26$ MHz, $\eta_q = 0.3$, the shielding parameters listed in Table 2, and Euler angles relating the two tensor orientations of (0°, 20°, 60°).

for this discrepancy could lie in a considerable reduction of the $\langle \Delta E \rangle$ transition energies characterizing the splitting between occupied and excited d orbitals in Co(Por)L_2 complexes, which would magnify the local asymmetry as viewed by the chemical shift. Theoretical calculations, however, predict for this crystal field an average value that is comparable to that observed for the simpler Co(III) complexes (16 000 cm^{-1}).[44] Furthermore these $\langle \Delta E \rangle$ values can be expected to remain essentially constant at least within our cobaltoporphyrin series, and yet the substantial increases in e^2qQ/h values displayed by the pyridine and isoquinoline complexes when compared to the imidazole

TABLE 3: Comparison of Shielding Anisotropies and Quadrupolar Couplings Measured for Different Hexacoordinated Cobalt Complexes[a]

compound	$\lvert\delta_{cs}^{zz} - \delta_{cs}^{iso}\rvert$ (ppm)	e^2qQ/h (MHZ)	ref
trans-[Coen$_2$Cl$_2$]cl·HCl·2H$_2$O	3100	72	18
[Co(NH$_3$)$_5$CN]Cl$_2$	1500	27	18
trans-[Coen$_2$(NO$_2$)$_2$]NO$_3$	200	13	18
Na$_3$[Co(NO$_2$)$_6$]	180	9	22
[Co(NH$_3$)$_6$]$_3$	≈0	3	20
Co(Por)Im$_2$[b]	1750	5	this work
Co(Por)MeIm$_2$[b]	1750	4	this work
Co(TPP)Py$_2$	1650	16.5	this work
Co(TPP)IsoQ$_2$	2500	26	this work

[a] Rounded to significant digits. [b] Averaged values (Tables 1 and 2).

ones are not accompanied by nearly as large a change in their $\{\delta_{cs}^{ii} - \delta_{cs}^{iso}\}_{i=x,y,z}$ tensor elements.

These results suggest that the ^{59}Co paramagnetic shielding in cobaltoporphyrins is being influenced by a mechanism that is not active in simpler Co(II) complexes. An obvious structural feature which is constant throughout the porphyrin series but absent from these simpler complexes is the presence throughout the former of an extensive aromatic orbital system. Conjugation and delocalization of the d metal electrons within this π system could provide a new mechanism affecting the ^{59}Co shielding paramagnetism that will be independent of the local asymmetry surrounding the cobalt site and unavailable to complexes possessing nonaromatic substituents. Indeed if ground and excited d orbitals were to lose some of their metallic character and become part of a larger aromatic system, the energies determining their mixing would cease to give given exclusively by the Co(III) crystal field and start reflecting instead the smaller $\langle\Delta E\rangle$ gap characterizing electrons within the porphyrin π system. Due to its macrocyclic origin such shielding contribution should be constant throughout a homologous porphyrin series and relatively independent of the local asymmetry at the metal site as viewed by the quadrupolar coupling, in agreement with the experimental observations. In an effort to find evidence regarding the existence of this mechanism, *ab initio* (Gaussian 94) and semiempirical (ZINDO) calculations of electronic distributions were carried out on model Co(Por)L$_2$ complexes and on simple hexacoordinate Co(III)L$_6$ (L = NH$_3$, NO$_2$) systems. These preliminary calculations confirmed that whereas in the latter complexes both the occupied and vacant d cobalt orbitals possess negligible ligand contributions, this ceases to be the case upon coordinating the metal to a porphyrin. A more complete account of these calculations as well as additional insight on this model arising from experimental Co(III)-phthalocyanine investigations, will be discussed in a future publication.

6. Conclusions

Solid state ^{59}Co NMR methods were used to characterize the metal sites in a series of synthetic hexacoordinated porphyrin complexes. Fast MAS and static determinations repeated at different fields and combined with numerical simulations afforded the isotropic and anisotropic chemical shifts as well as the quadrupolar coupling parameters for the different systems. When compared to previous solution NMR estimations, all cobalt sites were found to possess larger than expected shielding anisotropies and smaller than predicted electric field gradients. More interestingly, the relation between shielding and quadrupolar anisotropies observed throughout the porphyrins series deviated considerably from characteristic trends previously reported for simple octahedral cobalt complexes. Although the factors responsible for these deviations are yet unclear, an explanation consistent with the experimental observations was proposed based on interactions between the metal orbitals and the aromatic ligand orbitals. This model seems supported by simple quantum mechanical calculations, and if further verified could provide new insight into the electronic structure of metalloporphyrins. A definitive explanation of the observed effects will surely demand an improvement in the methods currently available for computing the electronic structure and NMR parameters of cobalt in complex systems, in conjunction with additional solid state ^{59}Co NMR determinations on extended series of compounds. Such efforts are currently under way.

Acknowledgment. We are grateful to Prof. Cynthia Jameson (University of Illinois at Chicago) for valuable discussions regarding the nature of chemical shifts and quadrupole couplings, to Mr. Peter Beverwyk (University of Illinois at Chicago) for his assistance in the quantum chemical calculations, and to Prof. Eric Oldfield (University of Illinois at Urbana−Champaign) for discussions on Mössbauer spectroscopy. This work was supported by the National Science Foundation through grants DMR-9420458 and CHE-9502644 (CAREER Award). A.M. acknowledges UIC for a Dean Fellowship; L.F. is a Camille Dreyfus Teacher−Scholar Awardee (1996−2001), Beckman Young Investigator (1996−1998); University of Illinois Junior Scholar (1996−1999); and Alfred P. Sloan Fellow (1997−2000).

References and Notes

(1) *Porphyrins and Metalloporphyrins*; Smith, K., Ed.; Elsevier: Amsterdam, 1976.
(2) *B$_{12}$*; Dolphin, D., Ed.; J. Wiley: New York, 1982.
(3) Mason, J. *Chem. Rev.* **1987**, *87*, 1299.
(4) Wehrli, F. W. *Annu. Rep. NMR Spectrosc.* **1979**, *9*, 201.
(5) Kidd, R. G. *Annu. Rep. NMR Spectrosc.* **1980**, *10A*, 28.
(6) Benn, R.; Rufinska, A. *Angew. Chem., Int. Ed. Engl.* **1986**, *25*, 861.
(7) Dechter, J. J. *Prog. Inorg. Chem.* **1985**, *33*, 393.
(8) Hagen, K. I.; Schwab, C. M.; Edwards, J. O.; Sweigart, D. A. *Inorg. Chem.* **1986**, *25*, 978.
(9) Hagen, K. I.; Schwab, C. M.; Edwards, J. O.; Jones, J. G.; Lawler, R.; Sweigart, D. A. *J. Am. Chem. Soc.* **1988**, *110*, 7024.
(10) Bang, H.; Cassidei, L.; Danford, H.; Edwards, J. O.; Hagen, K. I.; Krueger, C.; Lachowitz, J.; Schwab, C. M.; Sweigart, D. A.; Zhang, Z. *Magn. Reson. Chem.* **1989**, *27*, 1117.
(11) Cassidei, L.; Bang, H.; Edwards, J. O.; Lawler, R. G. *J. Phys. Chem.* **1991**, *95*, 7186.
(12) Bang, H.; Edwards, J. O.; Kim, J.; Lawler, R. G.; Reynolds, K.; Ryan, W. J.; Sweigart, D. A. *J. Am. Chem. Soc.* **1992**, *114*, 2843.
(13) Abragam, A. *The Principles of Nuclear Magnetism*; Oxford University Press: Oxford, UK, 1985.
(14) Spiess, H. W. In *NMR Basic Principles and Progress*; Diehl, P., Fluck, E., Kosfeld, R., Eds.; Springer-Verlag: New York, 1978; Vol. 15.
(15) Ramsey, N. F. *Phys. Rev.* **1950**, *78*, 699.
(16) Freeman, R.; Murray, G. R.; Richards, R. E. *Proc. R. Soc.* **1957**, *A242*, 455.
(17) Mehring, M. *High Resolution NMR in Solids*; Springer-Verlag: Berlin, 1983.
(18) Spiess, H. W.; Haas, H.; Hartmann, H. *J. Chem. Phys.* **1969**, *50*, 3057.
(19) Lourens, J. A.; Reynhardt, E. C. *Phys. Status Solidi (A)* **1972**, *11*, 739.
(20) Reynhardt, E. C. *Can. J. Phys.* **1974**, *52*, 1398.
(21) Eaton, D. R.; Buist, R. J.; Sayer, B. G. *Can. J. Chem.* **1987**, *65*, 1332.
(22) Chung, S. C.; Chan, J. C. C.; Au-Yeung, S. C. F.; Xu, X. *J. Phys. Chem.* **1993**, *97*, 12685.
(23) Hayashi, S. *Magn. Reson. Chem.* **1996**, *34*, 791.
(24) Balch, A. L.; Watkins, J. J.; Doonan, D. J. *Inorg. Chem.* **1979**, *18*, 1228.
(25) Eenzke, D.; Freude, F.; Frohlich, T.; Haase, J. *Chem. Phys. Lett.* **1984**, *111*, 171.
(26) Jannsen, R.; Veeman, W. S. *J. Chem. Soc., Faraday Trans.* **1988**, *84*, 3747.

(27) Ganapathy, S.; Schramm, S.; Oldfield, E. *J. Chem. Phys.* **1982**, *77*, 4360.
(28) Kundla, E.; Samoson, A.; Lippmaa, E. *Chem. Phys. Lett.* **1981**, *83*, 229.
(29) Cheng, J. T.; Edwards, J. C.; Ellis, P. D. *J. Phys. Chem.* **1990**, *94*, 553.
(30) Maricq, M. M.; Waugh, J. S. *J. Chem. Phys.* **1979**, *70*, 3300.
(31) Lefebvre, F.; Amoreux, J. P.; Fernandez, C.; Derouane, E. G. *J. Chem. Phys.* **1987**, *86*, 6070.
(32) Skibsted, J.; Nielsen, N. C.; Bildsøe, H.; Jakobsen, H. J. *Chem. Phys. Lett.* **1992**, *188*, 405.
(33) Herzfeld, J.; Berger, A. E. *J. Chem. Phys.* **1980**, *73*, 6021.
(34) Slichter, C. P. *Principles of Nuclear Magnetic Resonance*; Springer-Verlag: New York, 1990.
(35) Jameson, C. J. In *Multinuclear NMR*; Mason, J., Ed.; Plenum: New York, 1987; p 51.
(36) Jameson, C. J.; Gutowsky, H. S. *J. Chem. Phys.* **1964**, *40*, 1714.
(37) Chan, J. C. C.; Au-Yeung, S. C. F. *J. Chem. Soc., Faraday Trans.* **1996**, *92*, 1121.
(38) Townes, C. H.; Dailey, B. P. *J. Chem. Phys.* **1949**, *17*, 782.
(39) Lucken, E. A. C. *Nuclear Quadrupole Coupling Constants*; Academic Press: London, 1963.
(40) Hirschinger, J.; Granger, P.; Rosé, J. *J. Phys. Chem.* **1992**, *96*, 4815.
(41) Kirby, C. W.; Puranda, C. M.; Power, W. P. *J. Phys. Chem.* **1996**, *100*, 14618.
(42) Polam, J. R.; Shokhireva, T. K.; Raffii, K.; Simonis, U.; Walker, F. A. *Inorg. Chim. Acta*, in press.
(43) Kobayashi, H.; Maeda, Y.; Yanagawa, Y. *Bull. Chem. Soc. Jpn.* **1970**, *43*, 2342.
(44) Antipas, A.; Gouterman, M. *J. Am. Chem. Soc.* **1983**, *105*, 4896.